Experimental Investigation of Methane-Water and Methane-Brine IFT Measurements using Pendant Drop (rising bubble) Method

Aminu A. Yahaya[1], Emmanuel U. Akpan[2], Godpower C. Enyi[3], Ghasem G. Nasr[4], [5]Abubakar J. Abbas

[1] a.a.yahaya@edu.salford.ac.uk; [2] e.u.akpan@edu.salford.ac.uk; [3]g.c.enyi@salford.ac.uk; [4] g.g.nasr@salford.ac.uk; [5] a.j.abbas@salford.ac.uk

[1, 2, 3, 4, 5] Petroleum Technology and Spray Research Group, School of Computing, Science and Engineering, University of Salford, Manchester, United Kingdom, M5 4WT

Abstract

Gas hydrate formation involves low molecular gas mass transfer to a cage-like structure formed by water molecule under low temperature and high-pressure conditions. Gas hydrate is considered a problem if it develops along a pipeline. In order to solve the problem of gas hydrate formation in the pipeline, there is a need to understand the Interfacial Tension (IFT) behaviour at gas-water interface. This paper presents an experimental investigation of IFT of methane bubble in distilled water and varying concentration of salt (NaCl) using pendant drop (rising bubble) method. The results obtained shows that the IFT decreases with an increase in temperature and pressure. This decreasing trend shows that IFT existing at CH_4 – H_2O interface is a function of temperature and pressure. Additionally, the concentration of 2.9, 5.6, 8.2 and 10.7wt% NaCl resulted in an average increase of the IFT of the CH_4-H_2O system in 1.46, 2.57, 3.51 and 4.24 $mN.m^{-1}$ respectively.

Keywords: Gas hydrate, interfacial tension (IFT), multiphase system, brine concentration

1 Introduction

Considering the risk associated with blockages in a gas pipeline due to hydrate [1], [2], resulting from the natural gas flow with water under low temperature and high-pressure conditions [3]. It is essential to understand hydrate formation mechanisms, to prevent its formation along the pipeline. Hydrate formation is a process involving gas mass transfer to a cage-like structure formed by a water molecule. Interfacial Tension (IFT) working at the gas-water interface is one of the vital parameter controlling such transfer [4], [5]. Also, the dynamic of a two-phase system involving gas-water depends intensely on the temperature and pressure conditions [6], as well as IFT. The recent studies on hydrates mainly focused on predicting hydrate formation conditions [7]–[9], preventing and managing it when formed [2], [10]–[13].

The reported literature on the interfacial tension exhibited at the interface isolating a gaseous methane, and liquid water is limited. The interfacial tension data presently accessible in the

literature was obtained under limited pressure and temperature conditions. Sachs & Meyn [14] reported the response in the interfacial tension in the system methane – water due to pressure variation using pendant drop method (rising bubble mode) at 298.15K, for pressures ranges between 0.5 and 46.8 MPa. The interfacial tension measurement was performed only at 298.15K and pressure increases from 0.5 up to 46.8 MPa. Ren et al. [15] investigated methane – water, interfacial tension in systems containing a mixture of methane with five different compositions of carbon dioxide ranging from 20 – 80 mole%. The study employed same pendant drop technique as [14], and the measurements covered the temperature ranges from 298.15 to 373.15 K and pressure ranges from 1.0 to 30 MPa. This investigation was subsequently followed up by Yan et al. [16]. Using same pendant drop (rising bubble) method, investigated the effect of temperature, pressure and gas composition on interfacial tension of (methane + Nitrogen) – water and (Carbon dioxide + Nitrogen) – water. The experimental temperature and pressure ranges were 298 – 373 K and 1 – 30 MPa, respectively. Rushing et al. [17] measured dry gas-liquid interfacial tension and evaluated the effect of gas contaminant (Carbon dioxide and Nitrogen) on the gas-liquid interfacial tension behaviour using a pendant drop method, with computer-aided image processing and analysis. They investigated a high pressure and temperature ranges of 6.89 - 137.89 MPa and temperatures of 422 - 477.6 K, while methane-water and the methane-brine mixture were not considered at this condition, despite salts presents in the gas pipeline along the crates [18]. Khosharay & Varaminian [19] reported the interfacial tension of water with lower hydrocarbon alkane including water-methane, water-ethane, water-carbon dioxide, and water-propane systems using pendant drop method at temperatures from 284.15 to 312.15 K and pressures up to 6 MPa. Kashefi et al. [20] obtained interfacial tension data in methane – water and methane – brine using the pendant drop and bubble rise methods for temperatures ranging from 311 – 473 K and pressures up to 92 MPa. Yasuda et al. [6]reported the interfacial tension of water-methane system using pendant drop method at temperatures from 278.15 - 298.15 K and pressures up to 10 MPa. The study by [6] was followed up Hayama et al. [21], reported the interfacial tension of mixtures of methane with another hydrocarbon alkane (ethane and propane) at various proportion employing same techniques. The composition of their natural gas was 89.95% methane, 7.05% ethane and 3.00% propane and 95.0% methane, 3.5% ethane and 1.5% propane. These measurements were conducted at a pressure of up to 10 MPa and temperature between 283.2 K and 298.2 K, respectively. However, the investigations above did not cover a broader range of temperature and pressure and also no evidence of methane-brine systems except for [20]. Kashefi et al. [20] also failed to consider investigating the IFT below 311 K, which this present work seeks to address.

Additionally, the significance of gas bubble and their rise, due to buoyancy for different types of gas-liquid reactors have been investigated [23], [24] and they fail to consider the influence of the IFT of the gas bubble rise. Apart from the experimental investigation of interfacial tension working at gas – liquid and liquid-liquid interface, a thermodynamics-based theoretical approach to the nature of interfacial tension in water-methane and other related systems has been attempted by several research groups, and these can be found in [25]–[28]

Therefore, based on the literature surveyed as outlined above, this study aimed at investigating the interfacial tension in the methane – water system at temperatures ranges 298.15 – 313.15 K and pressures ranges 0.172 – 13.1 MPa. Pendant drop (rising bubble) method was used for conducting the present work, due to its convenience in dealing with the gas-liquid, closed, and a pressurised system similar to conditions found in most of the processing facilities.

2 Theory of Interfacial Tension

Interfacial tension of the methane bubble is determined from the profile of the bubble created using a radius of the curvature (R_0) and the shape factor (β) by the equation 1 & 2:

$$\gamma = \Delta\rho g \left(\frac{R_0^2}{\beta}\right) \quad (1)$$

and

$$\Delta\rho = \rho_{gas\ phase} - \rho_{liquid\ phase} \quad (2)$$

Where Δρ is the density difference between the continuous and risen bubble phase, g is the gravitational constant, R_0 is the radius of curvature at the hanging bubble apex, and β is the shape factor.

The bubble profile has been described using Young-Laplace equation, which is presented in a dimensionless form as shown in equation 3 - 5:

$$\frac{d\theta}{dS} = 2 - \beta Y - \frac{sin\theta}{X} \quad (3)$$

$$\frac{dX}{dS} = cos\theta \quad (4)$$

$$\frac{dY}{dS} = sin\theta \quad (5)$$

Fig. 1 illustrated the bubble with the descriptions of the x, y, s and θ.

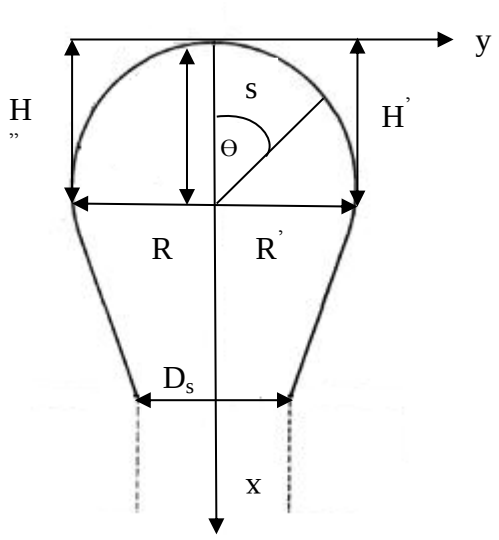

Fig. 1: Dimensions and symbols used

The parameter, s, is the distance along the drop profile from the drop apex, X, Y and S are dimensionless parameters made by dividing x, y, and s, respectively by R_0. H'' and H' are the distance from the centre of the curvature to the drop apex. A large number of theoretical dimensionless profiles were calculated for the whole possible β-range, from β = -0.55 to 10^{20} using Kutta-Merson's numerical integration algorithm with automatic step length adjustment. The maximum relative error was set to 10^{-4}. Each profile was measured mathematically by using cubic interpolation. In this way curves correlating the parameters β and R_0 with measurable parameters as indicated in Fig. ***1*** were produced, and these curves were fitted with linear polynomials by the method of least squares.

For pendant drops too short for the determination of D_S (D_S is the diameter at a distance D_E from the drop apex), the drop height (H), and the radius (R) is used. R is given as shown in equation 6:

$$R = \frac{D_E}{2} \tag{6}$$

D_E is the maximum diameter of the bubble from the bubble apex of methane gas. Equation 1 may be re-written in term of H as shown in equation 7 as:

$$\gamma = \Delta\rho g \left(\frac{H^2}{\beta}\right) \tag{7}$$

Where β is a transformed shape parameter. It is easily observed that H will have an upper limit because of the maximum hydrostatic pressure the surface tension may resist. When the drop becomes infinitely full, only one radius of curvature will be necessary, and the limiting

value of β is 2.0. Equation 7 is therefore much more convenient for small pendant bubbles. Another parameter B may derive from Equation 1 and 7 as a function of the ratio x = H/R as shown in equation 8 and 9 as:

$$B = \beta * \left(\frac{H}{R_0}\right)^2 = f(x) \quad (8)$$

$$\frac{H}{R_0} = g(x) \quad (9)$$

Combining equation 8 and 9 yields:

$$b = f(x)/g(x) \quad (10)$$

Therefore R_0 and β are determined for all values of β<1000 from the measured values of H and R from the profile and equations 9 and 10.

3 Experimental setup

A custom-assembled experimental device (as shown in Fig. 2) was used to perform IFT estimation tests through pendant bubble procedure and investigated images utilising Drop Image Advanced Analysis (DAA) Method. This section provides detail explanation of material, experimental setup and procedure.

3.1 Materials

The sample fluids utilised as part of the trials were research-grade methane gas provided by BOC Industrial Gases Co., Ltd., and distilled water prepared in our laboratory. The former having certified purity of 99.9% in mole fraction was used as received from the supplier. The latter was produced by treating tap water with a laboratory water distiller (D400 Distinction water still, Stuart Equipment). Fisher Scientific supplied the NaCl used for the brine preparation.

3.2 Apparatus and procedure

Fig. 2 shows the experimental setup used in the current work. The fundamental part of the rig was a cylindrical chamber made of stainless steel. The volume of the cell is 39 cm^3 and is fitted with a glass window to allow visual observation and a live recording of the shape of each risen bubble using a *rame-hart* camera. The temperature controller controlled the temperature of the chamber, using heating element mounted on the cell made from copper. A capillary tube, made of stainless-steel, 3.16 mm in outside diameter (O.D.), was inserted via the needle insertion hole at the bottom of the cell such that each bubble of methane suspended from the tip can be seen at the midpoint of the inside cell. The opposite end of the chamber's viewing window is the illuminating light source. Liquid water source (15 cm^3 stainless-steel

cylinder) is connected by the side of the chamber. Also, a platinum-wire resistance thermometer (Type K) was inserted into the cell from its side. The thermometer is located that its tip was only ~1mm away from the inside of the chamber. The uncertainty of the temperature measurement using this thermometer was estimated to be ±0.2 K. The inside pressure of the cell was control using a manual pump and the back-pressure regulator and was recorded using E-Zone pressure regulator with an estimated uncertainty of ±0.03 MPa.

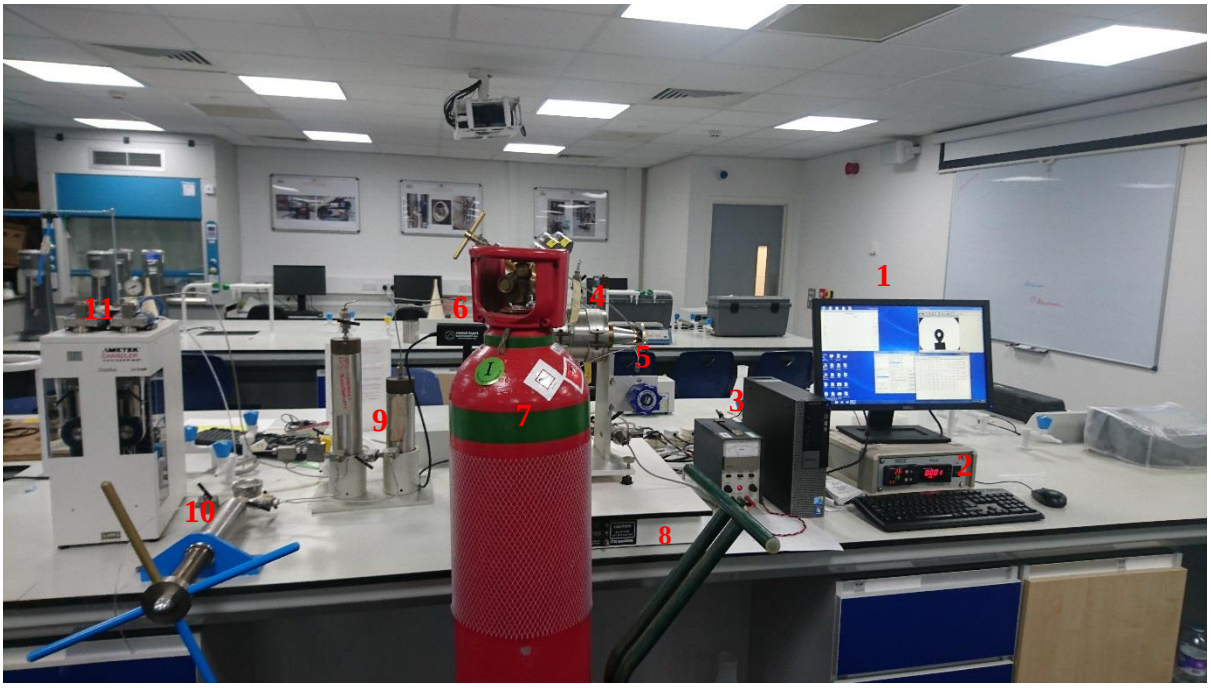

Fig. 2: Experimental set-up for IFT measurement (1-Data acquisition system; 2-Temperature and pressure recorder; 3-Illuminator; 4-IFT Measurement Chamber; 5-Back-pressure regulator; 6-Rame-hart Camera; 7-Methane cylinder; 8-Vibration control table; 9-water sample cylinder; 10-Manual pump; 11-Automatic pump)

Each trial for measuring the interfacial tension was commenced by filling the liquid sample cylinder with water sample using an automatic pump and then to the chamber via the sample cylinder. The manual pump was subsequently charged with the fluid sample after isolating the automatic pump. The pressure of the chamber was then adjusted to the desired pressure by using both manual pump and the back-pressure regulator. The methane source connected to the capillary tube mating valve was then used to form a rising bubble of the appropriate size at the tip of the capillary tube. The bubble was allowed to stand for 5-10 min to ensure that the bubble was thermally equilibrated with the surroundings. Images of the drop were then captured by the *rame-hart* camera and analysed using the Drop image advanced. Ten measurements were acquired for each image captured within 10sec at 1sec time interval between measurements. The average value of the interfacial tension values obtained from the bubble profile at each prescribed experimental pressure and temperature was regarded as the

interfacial tension value representative of the present work. As visual illustrations of such risen bubble images, Fig. 3 shows eight typical images obtained under significantly different temperature and pressure conditions.

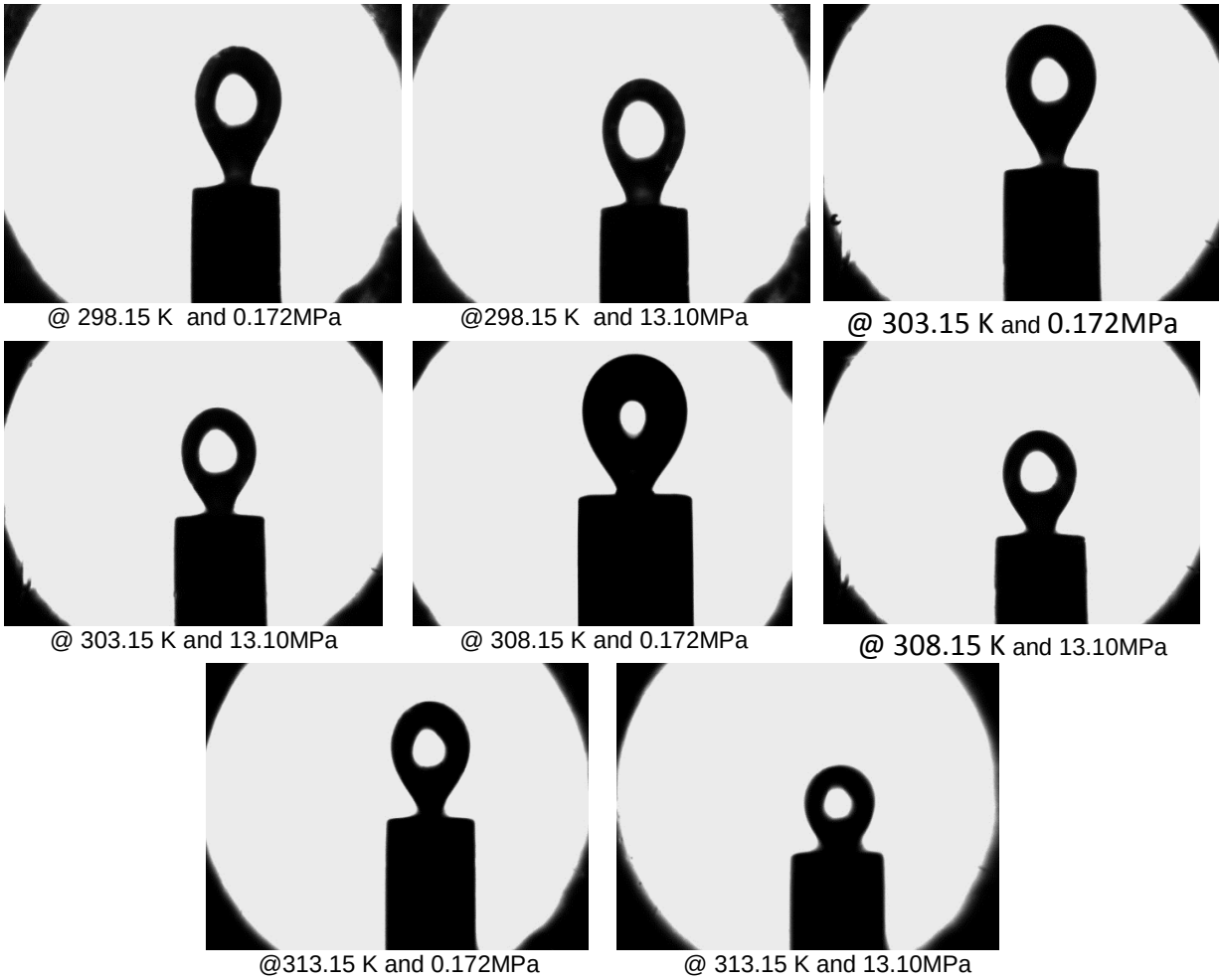

Fig. 3: Typical images of pendant drops captured at different temperature and pressure conditions

The measurements of the surface tension of water with air were also performed to affirm the dependability of this technique utilised for the present work. The analyses of the interfacial tensions were performed under five temperature conditions; i.e., 298.15, 303.15, 308.15 and 313.15 K.

A contour determines the pendant bubbles shape following algorithm, and the profile coordinates were used to determine the interfacial tension and area and volume of the drops or bubbles captured. The density of liquid water saturated with methane and that of gaseous methane was evaluated using REFPRO. The error analysis estimated the combined standard uncertainty of each interfacial tension value.

4 Results and Discussions

The experimental results obtained for the IFT of the methane-water system were measured at 298.15, 303.15, 308.15 and 313.15 K of temperature and pressure up to 13.10MPa. The

results obtained are plotted in Fig. 4. The validity of both the methodology and equipment used were assessed by comparison of the results obtained against literature data [6], [16], [19]. Additionally, the effect of salts was investigated by measuring the interfacial tension of methane-brine systems.

The brine sample used in the study contained 2.9, 5.6, 8.2 and 10.7% NaCl and the results obtained are plotted in Fig. 7, Fig. 8, Fig. 9 and Fig. 10. The results for methane-brine were compared against a literature [20]. These experiments were conducted to investigate the influence of pressure, temperature and salinity on the interfacial tension working at methane-water and methane-brine interface.

4.1 Methane-water

The experimental results of the present work showed a reduction of the interfacial tension with increasing pressure as can be seen in Fig. ***4*** and also Fig. ***6*** showed the corresponding decrease in IFT due to temperature though was not as pronounced as the pressure effect. Which could be as a result of the three pressures (0.172, 5.343 and 13.10MPa) chosen to see the impact of temperature and also the temperature ranges selected for the investigation. Moreover, this reduction seems to be more pronounced at a pressure ranges (3.62 – 13.1) MPa.

Even though, several data on methane-water IFT at wide range of pressures and temperatures available in the literature [6], [14], [15], [17], [19]–[21], [25], [29]–[32]. Only Khosharay & Varaminian [18]; Yan et al. [16]; and Yasuda et al. [6] measured isotherms are adequately close for correlation with the IFT data from the present work (see Fig. 5). As indicated in Fig. 5, the IFT values measured in this work are in reasonable agreement with the data from Yasuda et al. and Khosharay & Varaminian at a lower pressure up to 7.02MPa with an average deviation above 7.02MPa at T = 298.15K. However, there is significant disparity while compared to the data obtained by Yan et al. [16], within the investigated conditions and uncertainties of the present study.

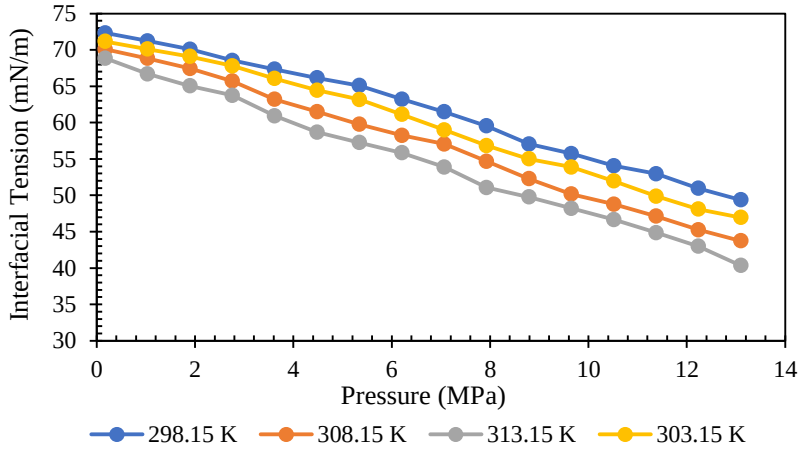

Fig. 4: IFT measurement for methane – liquid water at a constant temperature and various pressure

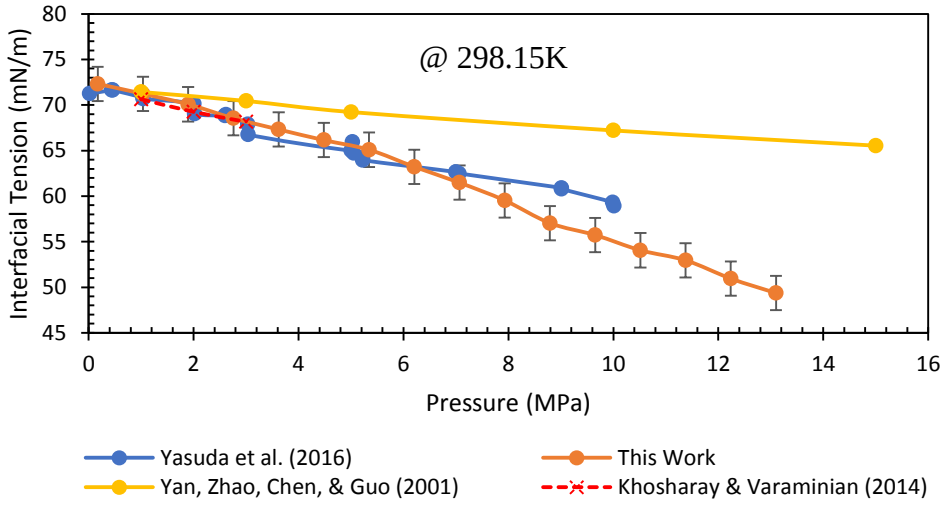

Fig. 5: A comparison of IFT-pressure diagrams for methane-water between this work and data obtained in some of the literature

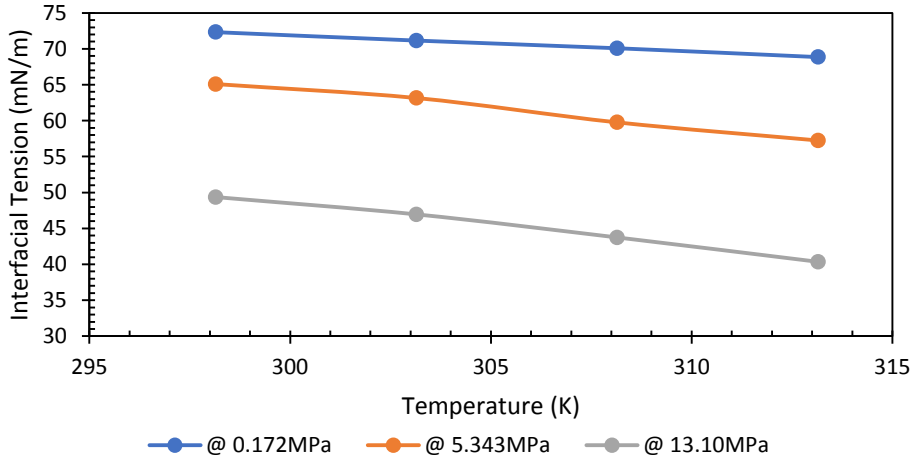

Fig. 6: Temperature effect on the methane-water IFT at constant pressure

4.2 Methane-Brine

The addition of salt resulted in a general increase of the interfacial tension values over the pressures and temperatures considered, as depicted in Fig. **7**, Fig. 8, Fig. 9 and Fig. 10. In

general, the presence of 2.9, 5.6, 8.2 and 10.7 wt% NaCl resulted in an average increase of the IFT in 1.46, 2.57, 3.51 and 4.24 $mN.m^{-1}$, respectively, when compared to the methane-water IFT. Furthermore, the change in IFT for the methane-brine system with pressure and temperature was found to be similar to that of the methane-water as mentioned above.

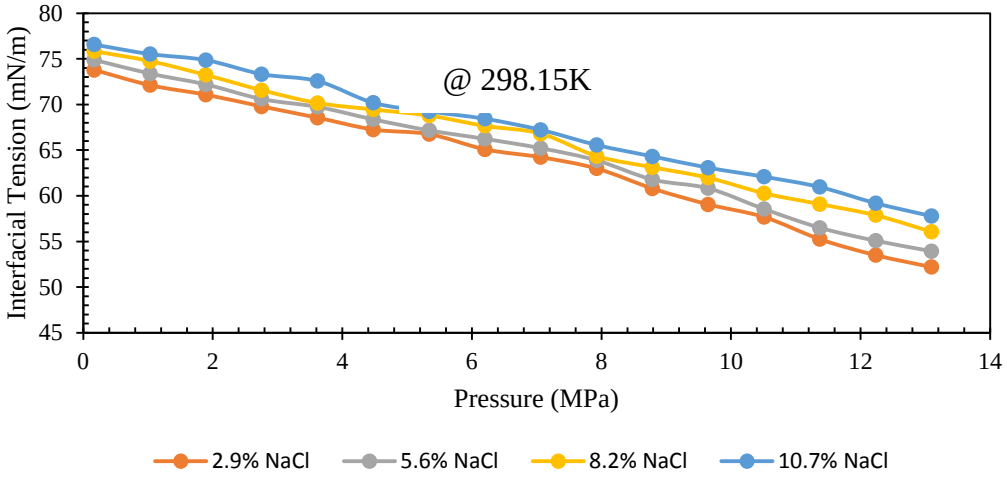

Fig. 7: IFT-pressure diagram for methane – brine measured at 298.15K and various concentration of NaCl

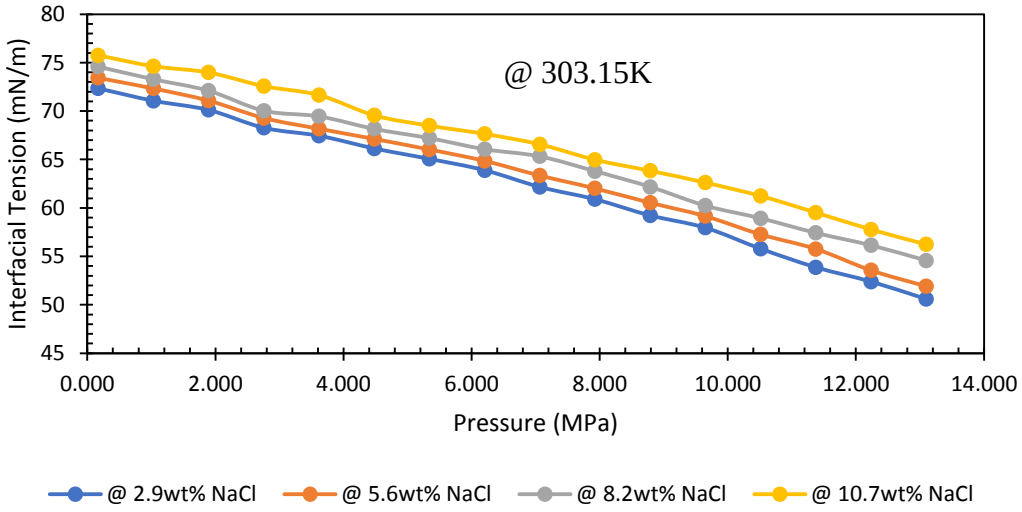

Fig. 8: IFT-pressure diagram for methane – brine measured at 303.15K and different concentration of NaCl

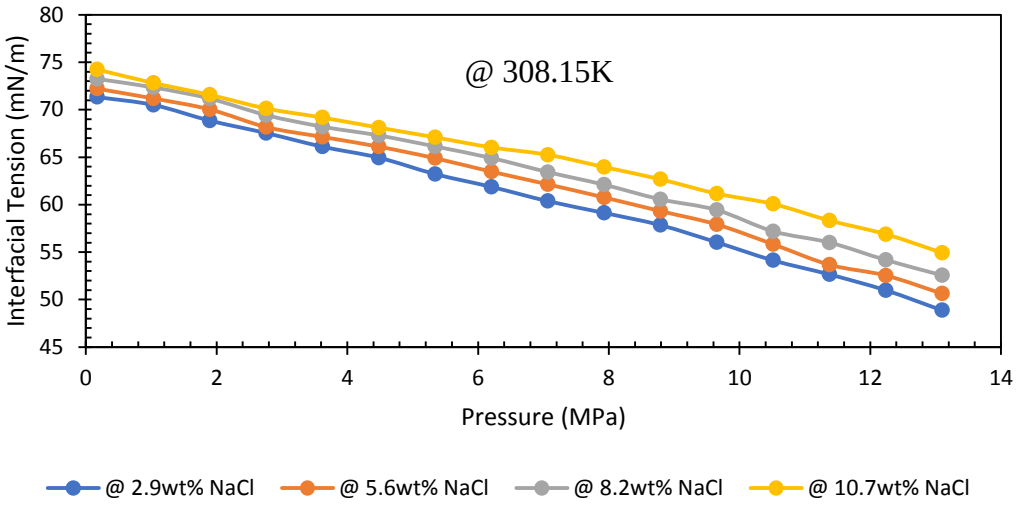

Fig. 9: IFT-pressure diagram for methane – brine measured at 308.15K and different concentration of NaCl

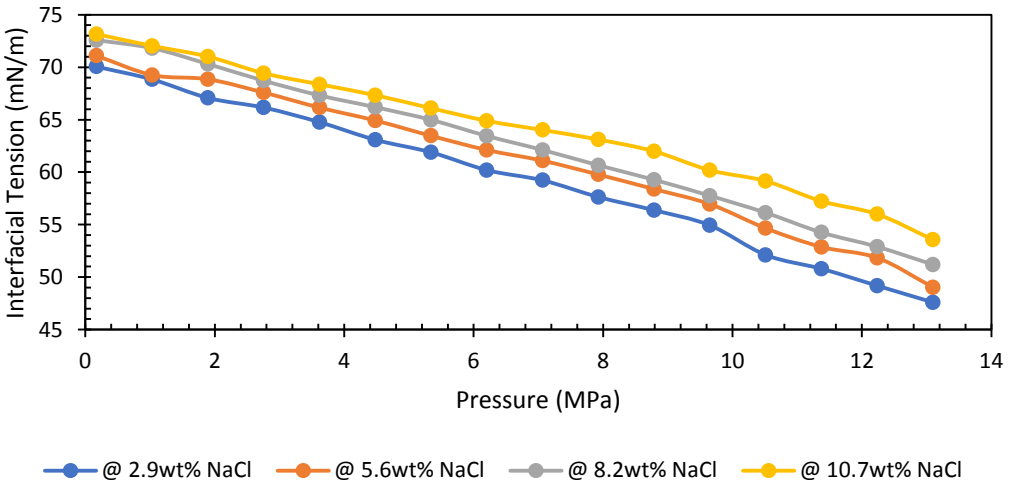

Fig. 10: IFT-pressure diagram for methane – brine measured at 313.15K and different concentration of NaCl

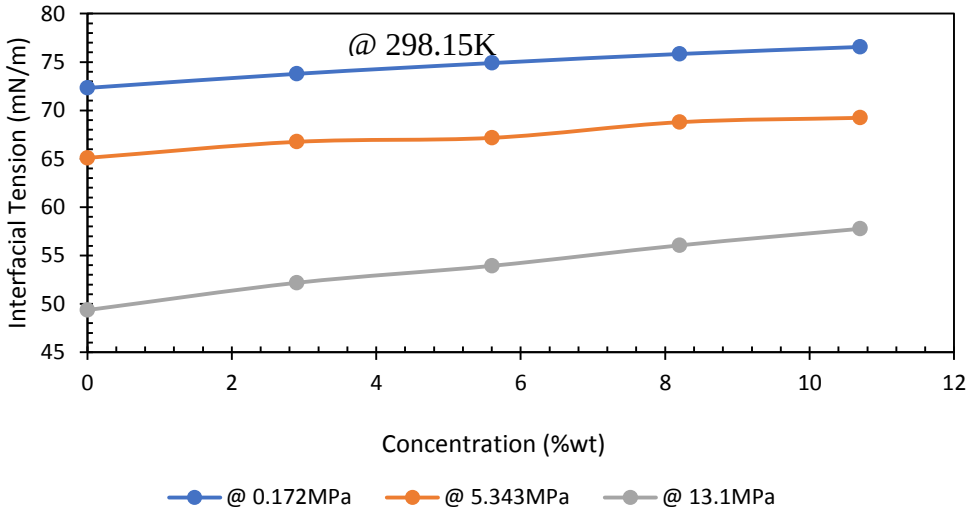

Fig. 11: Effect of NaCl concentration on methane – brine IFT measurement

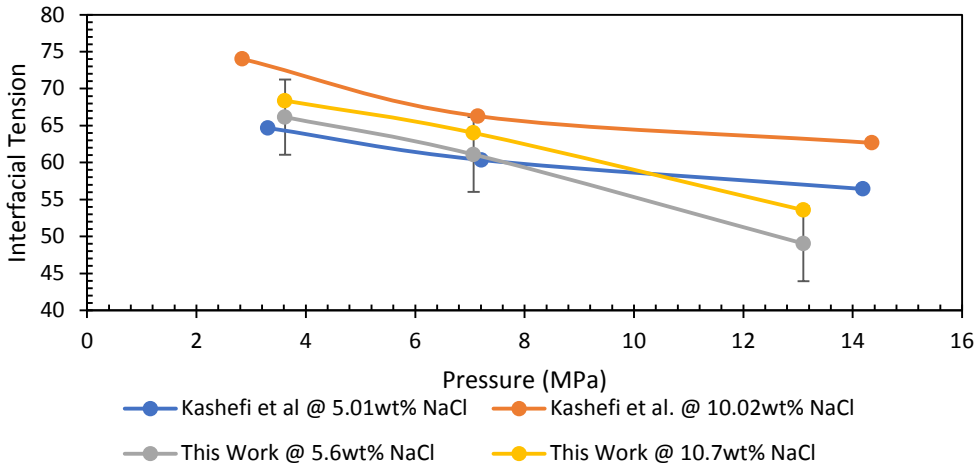

Fig. 12: A comparison of IFT-pressure diagrams for methane-brine between this work and data obtained in some of the literature

5 Conclusion

In the present work, pendant drop (risen bubble) method was used to measure the IFT for methane-water and methane-brine system for temperature range (298.18 to 313.15) K and Pressure (0.172 to 13.10) MPa. The effects of pressure, temperature, and salinity (NaCl) on the IFT were demonstrated. The results show the importance of IFT during mass transfer of methane into the water molecules. The presence of salt (NaCl) indicated a reduction of methane dissolution in the water thereby increasing the interfacial area of the methane bubble and hence the increase in the IFT. Additionally, the bubble size also affects the IFT values obtained. Both equipment and methodology were validated by comparison against methane-water and methane-brine in the literature.

6 References

[1] J. Boxall and E. May, 'Formation of gas hydrate blockages in under-inhibited conditions', in *Proceedings of the 7th International Conference on Gas Hydrates*, 2011.

[2] A. K. Sum, 'Prevention , Management , and Remediation Approaches for Gas Hydrates in the Flow Assurance of Oil / Gas Flowlines', in *Offshore Technology Conference*, 2013.

[3] C. A. Koh, E. D. Sloan, A. K. Sum, and D. T. Wu, 'Fundamentals and applications of gas hydrates.', *Annual review of chemical and biomolecular engineering*, vol. 2, pp. 237–57, Jan. 2011.

[4] M. Zarifi, J. Javanmardi, H. Hashemi, A. Eslamimanesh, and A. H. Mohammadi, 'Experimental Study and Thermodynamic Modelling of Methane and Mixed C1 + C2 + C3 Clathrate Hydrates in the Presence of Mesoporous Silica gel', *Fluid Phase Equilibria*, vol. 423, pp. 17–24, Mar. 2016.

[5] S. Hall, A. W. Pacek, A. J. Kowalski, M. Cooke, and D. Rothman, 'The effect of scale and interfacial tension on liquid-liquid dispersion in in-line Silverson rotor-stator mixers', *Chemical Engineering Research and Design*, vol. 91, no. 11, pp. 2156–2168, 2013.

[6] K. Yasuda, Y. H. Mori, and R. Ohmura, ‘Interfacial tension measurements in water−methane system at temperatures from 278.15 K to 298.15 K and pressures up to 10 MPa’, *Fluid Phase Equilibria*, vol. 413, pp. 170–175, 2016.

[7] J. Boxall, S. Davies, C. A. Koh, and E. D. Sloan, ‘Predicting When and Where Hydrate Plugs Form in Oil-Dominated Flowlines’, *SPE Projects Facilities & Construction*, vol. 4, no. 3, pp. 5–8, 2009.

[8] S. O. Salufu and P. Nwakwo, ‘New Empirical Correlation for Predicting Hydrate Formation Conditions’, *SPE*, no. August, pp. 1–18, 2013.

[9] R. E. T. Meindinyo, T. M. Svartaas, T. N. Nordbø, and R. Bøe, ‘Gas hydrate growth estimation based on heat transfer’, *Energy and Fuels*, vol. 29, no. 2, pp. 587–594, 2015.

[10] N. Ando, Y. Kuwabara, and Y. H. Mori, ‘Surfactant effects on hydrate formation in an unstirred gas/liquid system: An experimental study using methane and micelle-forming surfactants’, *Chemical Engineering Science*, vol. 73, pp. 79–85, 2012.

[11] E. F. May, R. Wu, M. a. Kelland, Z. M. Aman, K. a. Kozielski, P. G. Hartley, and N. Maeda, ‘Quantitative kinetic inhibitor comparisons and memory effect measurements from hydrate formation probability distributions’, *Chemical Engineering Science*, vol. 107, pp. 1–12, 2014.

[12] H. Sharifi, J. Ripmeester, V. K. Walker, and P. Englezos, ‘Kinetic inhibition of natural gas hydrates in saline solutions and heptane’, *Fuel*, vol. 117, pp. 109–117, 2014.

[13] N. Daraboina, S. Pachitsas, and N. von Solms, ‘Experimental validation of kinetic inhibitor strength on natural gas hydrate nucleation’, *Fuel*, vol. 139, pp. 554–560, 2015.

[14] W. Sachs and V. Meyn, ‘Pressure and temperature dependence of the surface tension in the system natural gas/water’, *Colloids and Surfaces A: Physicochemical and Engineering Aspects*, vol. 94, pp. 291–301, 1995.

[15] Q. Y. Ren, G. J. Chen, W. Yan, and T. M. Guo, ‘Interfacial tension of (CO2 + CH4) + water from 298 K to 373 K and pressures up to 30 MPa’, *Journal of Chemical and Engineering Data*, vol. 45, no. 4, pp. 610–612, 2000.

[16] W. Yan, G.-Y. Zhao, G.-J. Chen, and T.-M. Guo, ‘Interfacial Tension of (Methane + Nitrogen) + Water and (Carbon Dioxide + Nitrogen) + Water Systems’, *J. Chem. Eng. Data*, vol. 46, pp. 1544–1548, 2001.

[17] J. A. Rushing, K. E. Newsham, K. C. Van Fraassen, S. a Mehta, and G. R. Moore, ‘Laboratory Measurements of Gas-Water Interfacial Tension at HP/HT Reservoir Conditions’, *CIPC/SPE Gas Technology Symposium 2008 Joint Conference*, 2008.

[18] H. Fang, B. Brown, and S. Nesic, ‘High salt concentration effects on CO2 corrosion and H2S corrosion’, in *NACE International Corrosion Conference & EXPO*, 2010, no. 10276, pp. 1–29.

[19] S. Khosharay and F. Varaminian, ‘Experimental and modeling investigation on surface tension and surface properties of (CH4 + H2O), (C2H6 + H2O), (CO2 + H2O) and (C3H8 + H2O) from 284.15 K to 312.15 K and pressures up to 60 bar’, *International Journal of Refrigeration*, vol. 47, pp. 26–35, 2014.

[20] K. Kashefi, L. M. C. Pereira, A. Chapoy, R. Burgass, and B. Tohidi, ‘Measurement

and modelling of interfacial tension in methane/water and methane/brine systems at reservoir conditions', *Fluid Phase Equilibria*, vol. 409, pp. 301–311, 2016.

[21] H. Hayama, K. Fukuzawa, K. Yasuda, and R. Ohmura, 'Interfacial tension between (methane+ethane+propane) gas mixture and water from 283.2K to 298.2K under up to 10MPa', *The Journal of Chemical Thermodynamics*, vol. 108, pp. 71–75, 2017.

[22] K. Kashefi, C. Pereira, L. Manuel, A. Chapoy, R. W. Burgass, and T. K. Bahman, 'Measurement and modelling of interfacial tension in methane/water and methane/brine systems at reservoir conditions', *Fluid Phase Equilibria*, vol. 409, pp. 301–311, 2016.

[23] A. a Kulkarni and J. B. Joshi, 'Bubble Formation and Bubble Rise Velocity in Gas - Liquid Systems : A Review', *Industrial & Engineering Chemistry Research*, vol. 44, pp. 5873–5931, 2005.

[24] J. Zawala, D. Kosior, and K. Malysa, 'Formation and influence of the dynamic adsorption layer on kinetics of the rising bubble collisions with solution/gas and solution/solid interfaces', *Advances in Colloid and Interface Science*, vol. 222, pp. 765–778, 2015.

[25] K. A. G. Schmidt, G. K. Folas, and B. Kvamme, 'Calculation of the interfacial tension of the methane-water system with the linear gradient theory', *Fluid Phase Equilibria*, vol. 261, no. 1–2, pp. 230–237, 2007.

[26] O. G. Nino-Amezquita, S. Enders, P. T. Jaeger, and R. Eggers, 'Measurement and Prediction of Interfacial Tension of Binary Mixtures', *Industrial & Engineering Chemistry Research*, vol. 49, no. 2, pp. 592–601, 2010.

[27] L. Zhao, S. Lin, J. D. Mendenhall, P. K. Yuet, and D. Blankschtein, 'Molecular dynamics investigation of the various atomic force contributions to the interfacial tension at the supercritical CO2-water interface', *Journal of Physical Chemistry B*, vol. 115, no. 19, pp. 6076–6087, 2011.

[28] A. Chapoy, H. Haghighi, R. Burgass, and B. Tohidi, 'On the phase behaviour of the (carbon dioxide+water) systems at low temperatures: Experimental and modelling', *The Journal of Chemical Thermodynamics*, vol. 47, pp. 6–12, Apr. 2012.

[29] S. Khosharay, 'Linear gradient theory for modeling investigation on the surface tension of (CH4+H2O), (N2+H2O) and (CH4+N2)+H2O systems', *Journal of Natural Gas Science and Engineering*, vol. 23, pp. 474–480, 2015.

[30] M. Ghorbani and A. H. Mohammadi, 'Effects of temperature, pressure and fluid composition on hydrocarbon gas - oil interfacial tension (IFT): An experimental study using ADSA image analysis of pendant drop test method', *Journal of Molecular Liquids*, vol. 227, pp. 318–323, 2017.

[31] B. Z. Peng, C. Y. Sun, P. Liu, Y. T. Liu, J. Chen, and G. J. Chen, 'Interfacial properties of methane/aqueous VC-713 solution under hydrate formation conditions', *Journal of Colloid and Interface Science*, vol. 336, no. 2, pp. 738–742, 2009.

[32] C. Jho, D. Nealon, S. Shogbola, and A. D. King Jr., 'Effect of Pressure on the Surface Tension of Water: Adsorption of Hydrocarbon Gases and Carbon Dioxide on Water at Temperatures between 0 and 50 C', *J. Colloid Interface Sci.*, vol. 65, no. 1, pp. 141–154, 1978.